

## **ANISOTROPIC- MAGNETORESISTANCE INTEGRATED SENSORS**

S. Andreev\*, P. Dimitrova

Institute of Solid State Physics, Bulgarian Academy of Sciences, 72 Tzarigradsko  
Chaussee Blvd., 1784 Sofia, Bulgaria

In this paper, a short overview is presented of the most widely used types of solid state magnetic sensor. These sensors are applied in many areas, such as the measurement of magnetic fields and in compasses, angle/position sensors and current sensing. Hall effect, AMR (Anisotropic Magnetoresistance-effect) and GMR (Giant Magnetoresistance-effect) sensors are the most frequently used. In spite of the later appearance of the GMR structures, AMR sensors are still preferred in cases when high sensitivity, flexibility of design and compatibility with standard microelectronics technology are needed. A description of the basic mechanisms of the normal AMR effect and of the so-called "barber pole" effect is presented, and some of the main problems that have to be solved when designing and producing AMR devices are underlined. A model is proposed for the estimation of the effectiveness of real barber pole structures. Experimental results are reported and discussed, concerning the design and production of single-stripe resistors and barber pole bridges, based on a technology with magnetization after annealing. Conclusions are drawn about the compatibility of this technology with CMOS technology.

(Received December 9, 2004; accepted January 26, 2005)

*Keywords:* AMR, Thin films, Magnetic sensors

### **1. Introduction**

Several types of solid state magnetic sensor are used in practice for measuring magnetic fields and for automation. It seems that until the last few years, Hall-effect sensors were the most widely accepted. However, they work at relatively high fields (lower limit around 1 mT = 10 Oe) and require a device orientation perpendicular to the plane of the magnetic field, which is not convenient in many applications. The AMR (Anisotropic magnetoresistance) sensors that will be discussed below work in the range 1 nT to several mT; 0.01 Oe to several tens of Oe. They are implemented by a relatively simple technology and are widely used for the measurement of magnetic fields and also for automation. GMR (Giant Magnetoresistance) devices emerged recently, and currently gain new applications. They work in the range 100 nT to over 100 T, and are preferred for capturing stronger (and especially very strong) magnetic fields. However, they require more complex and sophisticated technology.

AMR sensors are still preferred in cases where high sensitivity, flexibility of the design and compatibility with standard microelectronics technology are needed [1-5].

### **2. Description of the key mechanisms**

The AMR effect is based on the fact that some ferromagnetic materials demonstrate a dependence of their resistivity on the angle between the direction of the current flow and the direction of their magnetization. The microscopic theory of this dependence is founded on the larger

---

\* Corresponding author: sandreev@issp.bas.bg

probability of s-d scattering for electrons travelling parallel to the magnetization [6-8]. Thus, the resistivity has its maximum value for a current flowing along the direction of magnetization, and its minimum value for current flow in perpendicular direction. When such a material is deposited as a well ordered thin film, it exhibits one only “easy axis” of magnetization in the plane of the film, and is spontaneously magnetized along this axis (two opposite polarities of the vector of magnetization are permitted along the axis). In a long stripe cut from such film along its “easy axis” (for instance by photolithography) the current would flow in parallel with the magnetization and the stripe would demonstrate its maximum resistance. Applying an external magnetic field of a certain magnitude  $H$ , directed perpendicular to the “easy axis”, would result in a rotation of the vector of magnetization  $\mathbf{M}$  around its initial position at some angle  $\theta$ , and a decrease in the resistance. Hence, such a structure could be used as a sensor of the perpendicular external field. The relation between the resistivity  $\rho$  and the angle  $\theta$  is expressed by the so-called Voight-Thomson formula:

$$\rho(\theta) = \rho_t + \Delta\rho \cos^2 \theta \quad (1)$$

where,  $\rho_t$  is the transverse resistivity in the direction perpendicular to the easy axis,  $\rho_l$  is the resistivity along the easy axis, and  $\Delta\rho$  is the addition to  $\rho_t$  in the direction of  $\rho_l$ , due to the AMR effect (in fact at  $\theta = 0$  Eq. 1 is reduced to  $\rho_l = \rho_t + \Delta\rho$ ). Thus, Eq. 1 is a correct description of the presence of an additional amount of resistivity (due to additional scattering mechanisms) in the direction parallel to the magnetization. However, for practical purposes it is more convenient to transform Eq. 1 into

$$\rho(\theta) = \rho_l + \Delta\rho \sin^2 \theta \quad (2)$$

because  $\rho_l$  is a practically measured quantity (the resistance/resistivity of a thin-film stripe without an applied external magnetic field). Then, the quantity  $\Delta\rho/\rho = (\rho_l - \rho_t)/\rho_l$  (the magnetoresistivity coefficient of the material) is used to describe the relative change of the measured resistances as follows:

$$\frac{\Delta R(H)}{R} = -\left(\frac{\Delta\rho}{\rho}\right) \sin^2 \theta \quad (3)$$

where  $R$  is the resistance measured at  $H=0$ , and  $\Delta R(H) = R(H) - R$  is the change of the resistance at a certain  $H \neq 0$ .

In practice, the angle  $\theta$  is usually not known, and the most important aspect is the direct dependence of  $\Delta R/R$  on the applied external magnetic field. This dependence can be derived from the expression for the free energy of the system:

$$W = -\mu_0 M H_x \sin \theta - \mu_0 M H_y \cos \theta + \frac{1}{2} \mu_0 M H_k \sin^2 \theta \quad (4)$$

where  $W$  is the free energy,  $H_x$ ,  $H_y$  are the components of the vector of the external magnetic field applied in the x-y plane of the thin film,  $M$  is the magnetization of the film and  $H_k$  is a characteristic field for the anisotropy. The first two terms in Eq. 4 represent the magnetostatic energy of the system, and the third term accounts for the anisotropy energy.

When the anisotropy axis is directed along the y-axis and the external field is applied perpendicular to it ( $H_x \neq 0$ ,  $H_y = 0$ ), minimizing of Eq. 4 through  $dW/d\theta = 0$  results finally in

$$\sin \theta = \frac{H_x}{H_k} \quad (5)$$

and from Eq. 3 we obtain

$$\frac{\Delta R(H)}{R} = -\frac{\Delta \rho}{\rho} \left( \frac{H_x}{H_k} \right)^2 \text{ and } R(H) = R - R \frac{\Delta \rho}{\rho} \left( \frac{H_x}{H_k} \right)^2. \quad (6)$$

Still, in the presence of a longitudinal component  $H_y \neq 0$  and for relatively small values of  $\theta$  (up to around  $30^\circ$ ) the following expressions could be derived as good approximations:

$$\frac{\Delta R(H)}{R} = -\frac{\Delta \rho}{\rho} \left( \frac{H_x}{H_k + H_y} \right)^2 \text{ and } R(H) = R - R \frac{\Delta \rho}{\rho} \left( \frac{H_x}{H_k + H_y} \right)^2 \quad (7)$$

The expected dependence of the relative change of the resistance  $R(H)/R$  on the ratio  $H_x / H_k$  is illustrated in Fig. 1. At larger magnetic fields there are significant discrepancies between this parabolic dependence and the experimental data (Fig. 2), but at relatively small fields it is followed exactly, as shown Fig. 3 [1]. Based on this, one can calculate  $H_k$  from Eq. 6 and from a parabolic function fitting the experimental data for small fields (several Oe).

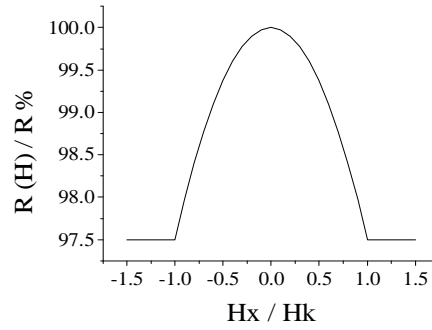


Fig. 1. Dependence of the relative change of the resistance on  $H_x/H_k$ .

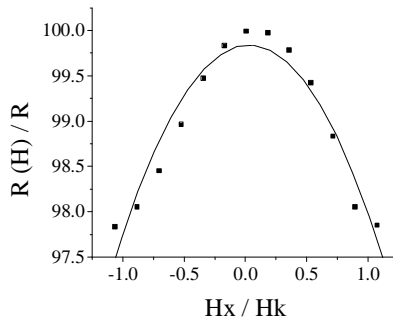


Fig. 2. Fitting of the dependence  $R(H)/R$  on  $H_x/H_k$  (line-fitted curve; dots-experimental data).

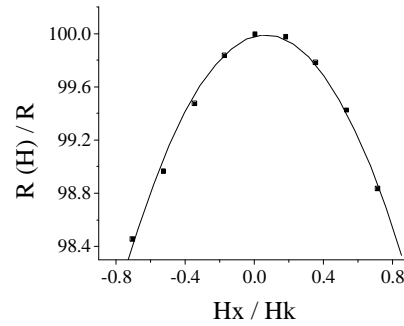


Fig. 3. Fitting of the dependence  $R(H)/R$  on  $H_x/H_k$  for small fields (line-fitted curve; dots-experimental data).

Devices based on the mechanism described above are used in various applications. However, they suffer from a significant drawback – they sense the value of the external field but not its polarity (N-S or S-N). In many applications (for instance angle measurements), sensing the polarity of the field is crucial. For this reason, several ways have been proposed to solve the problem. One widely used solution is based on the so-called “barber pole” effect [9-11]. In this case, the current is forced to flow not along the stripe but at  $45^\circ$  with respect to its axis. At the initial position ( $H=0$ ), the angle between the current flow and the magnetization is  $\theta = 45^\circ$ , and the resistance has a mean value (between the maximum and the minimum). Rotation of the magnetization to one side around the initial position results in a decrease in  $\theta$  and an increase in the

resistance. Rotation to the other side has the opposite effect. Thus, the polarity of the measured field is already recognizable. The inclination of the current flow with respect to the geometric axis of the stripe is achieved by the deposition over the stripe of shorting bars inclined at an angle  $\beta = 45^\circ$  to the geometrical axis, and at some distance between them as shown in Fig. 4. For these shorting bars, a low resistivity material is used (for instance Al or Au) and their thickness should be large enough to provide an effective shunting of the under-lying permalloy film. Special measures have to be taken to provide a good enough contact between the shorting bars and the permalloy layer. The use of an intermediate adhesive layer (for instance Ti) is recommended.

The resulting response  $R(H)/R$  on  $H_x / H_k$  is shown in Fig. 5. The curve of the response is anti-symmetric with respect to the polarity of the field, and a linear part featuring high sensitivity is observed around the zero point.

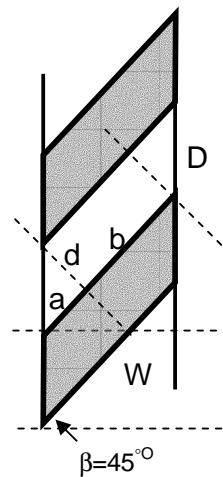


Fig. 4. Barber-pole structure with shorting bars (W- width of the stripe; D-distance between two shorting bars; a- effective length of the border area; b- effective length of the BP area).

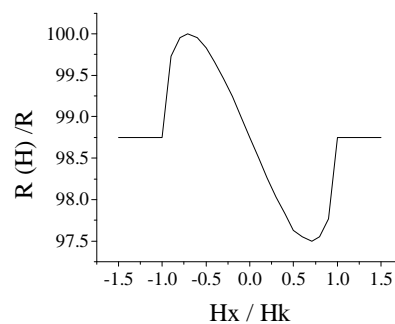


Fig. 5. Dependence of the relative change of the resistance on  $H_x/H_k$  for a barber pole magnetoresistor.

A major problem is the temperature dependence of the resistivity of the material. Our studies of a single-path magnetoresistor of permalloy have shown that a resistor of nominal value  $700 \Omega$  changes its value with temperature at a rate of around  $3.3 \Omega/^\circ\text{C}$ . This is in agreement with reference data for the material. In practice, such variations are comparable to the response signal. When reading information, this is not a problem because temperature changes are slow and the AC component of the signal is easily derived. However, it is a big problem when measuring constant or slowly varying magnetic fields. Wheatstone-bridge circuits are usually applied to overcome this difficulty. Each arm of such a bridge consists of one active and one inactive (for instance shielded) magnetoresistor. The barber pole effect offers the excellent possibility of including into the arms of

the bridge resistors with opposite responses to the polarity of the field (depending on the angle  $\pm 45^\circ$  between the shorting bars and the axis of the stripe. In this arrangement, the total response is four times greater than that of one resistor taken individually.

### 3. Modelling the efficiency of the “barber pole” structure

Two considerations connected with the geometry of “barber pole” structures strongly affect their performance. One of them is the efficiency of the shunting bars. As mentioned previously, low resistivity materials have to be used for them. They should be as thick as possible, and special measures have to be taken to provide good enough contacts between the shorting bars and the permalloy layer. However, these contacts operate under very demanding conditions (the voltage drop to be shunted by one contact is around 1mV or less) and have to be very reliable (one bridge structure contains several thousands of contacts). Usually the designer’s rules prescribe that these contacts should be as narrow as possible. Dibbern, from Philips (as cited in [1]), recommends a value of 4  $\mu\text{m}$ . However, the capacity of the technology to implement narrow contacts should be assessed carefully, in order to meet the requirements discussed above. On the other hand, wider contacts are related to wider parts of the permalloy between them. Here comes the second consideration. The efficiency of the barber pole structure is strongly affected by the so-called border effect. It is due to the non-uniformity of the electric field in the permalloy near to the borders of the stripe (the triangle area in Fig. 4). In this region, the current does not flow strictly at  $45^\circ$  with respect to the axis of the stripe. These areas behave partially like barber pole structures and partially like simple magnetoresistive structures without a barber pole. The final result is a reduction and deformation of the output signal. In general, the total area of these regions should be minimized, by proper layout design. Here, the most simple and evident consideration is that for a given width  $w$  of the stripe the smaller the distance between two shorting bars (which also means narrower bars) – the smaller the area of the border regions. The conclusion can be drawn that one has to make a trade off between the requirements for 100% working contacts and for minimized areas of the border regions.

Incorrectly functioning shorting bars and large-area border regions lead to the same result – mixing of the barber pole (BP) mode of operation with the usual magnetoresistor mode (MR). For this reason and for assessment of the risk when making a choice of the width of the shorting bars and the distance between them, a model is proposed mixing the BP and MR modes in two ways: serial and parallel.

In the serial part of the model, a stripe with resistance  $R$  and length  $L$  is represented as two resistors  $R_{BP}$  and  $R_{MR}$  connected in series.  $R_{BP}$  represents the total resistance of the parts of the stripe where all contacts work properly and the BP mode is 100% efficient. On the other hand,  $R_{MR}$  is the total resistance of the parts with non-functioning shunts (MR mode). It is accepted in the model that the widths of the bars and the distances between them are equal ( $D$  in the Fig. 4). However, the choice of a different ratio does not affect the final conclusions. Having this in mind, and considering the length of these parts of the stripe, one has to take into account that equal length parts with working contacts have a four times smaller resistance than the permalloy by itself (partially because they are shunted and partially due to the current flowing at  $45^\circ$ ).

Results from this modelling are presented in Figs. 6, 7 and 8, for different percentages of working contacts. In the exemplary case it is accepted that the resistance of the permalloy stripe at  $H_x = 0$  is  $R(0) = 1025 \Omega$ . It is further supposed that some percentage of the length of the stripe works in BP mode and the rest in MR mode. In the captions to the figures, it is noted how  $R(0)$  is reduced by increasing the fraction of  $L$  ( $L_{BP}$ ) working in BP mode. In fact, it is expected that in this particular case  $R(0)$  will be reduced to  $256.25 \Omega$ , for 100% BP mode. From Fig. 6, it is seen that  $L_{BP} = 0.5 L$  only slightly affects the original MR mode. At  $L_{BP} = 0.75 L$  (Fig. 7), the dependence of  $\Delta R$  on  $H_x$  is asymmetric but still has the shape of the MR response. At  $L_{BP} = 0.90 L$  (Fig. 8) this dependence is a strongly distorted BP response. For even greater values, it rapidly changes to the anti-symmetric shape of the BP response.

In the parallel part of the model, each active (not shunted) segment of the permalloy layer is represented by two elements connected in parallel - a BP element (where the current is flowing

strictly at  $45^\circ$  with respect to the axis of the stripe) and an irregular MR element (the border area). Each of these is represented by its conductance ( $g_{BP}$  and  $g_{MR}$  respectively).

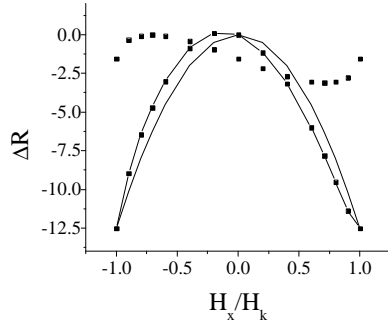


Fig. 6. Modelling serially mixed BP and MR effects.  $L_{BP} = 0.5L$  (line-  $\Delta R_{MR}$ ; dots -  $\Delta R_{BP}$ ; dotted line -  $\Delta R$ ).  $R(0) = 639.1\Omega$ .

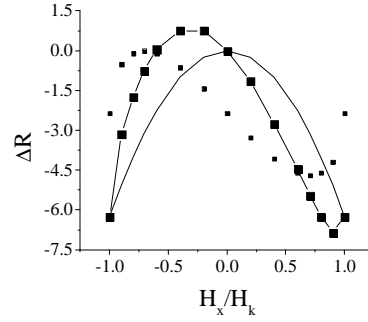


Fig. 7. Modelling serially mixed BP and MR effects.  $L_{BP} = 0.75L$  (line-  $\Delta R_{MR}$ ; dots -  $\Delta R_{BP}$ ; dotted line -  $\Delta R$ ).  $R(0) = 446.1\Omega$ .

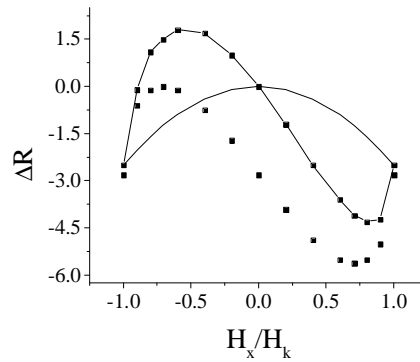


Fig. 8. Modelling serially mixed BP and MR effects.  $L_{BP} = 0.90L$  (line-  $\Delta R_{MR}$ ; dots -  $\Delta R_{BP}$ ; dotted line -  $\Delta R$ ).  $R(0) = 330.0\Omega$ .

The entire stripe is considered as a system consisting of such  $g_{BP}/g_{MR}$  pairs connected in series. Here, the ratio  $D/W$  is a measure of the disturbing factor (the border effect). As an example, the response of  $g_{BP}$ ,  $g_{MR}$  and the change of the total resistance  $\Delta R$  to the applied field for the case  $D/W = 2/3$  is shown in Figs. 9 and 10.

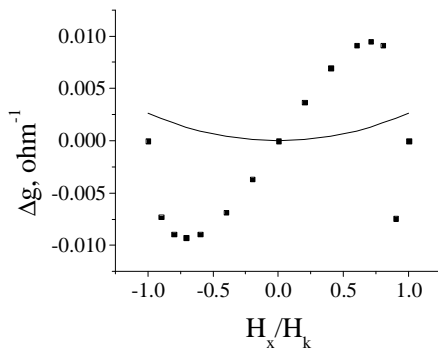


Fig. 9. Modeling mixed in parallel BP and MR effects. (line -  $\Delta g_{MR}$ ; dots -  $\Delta g_{BP}$ ).

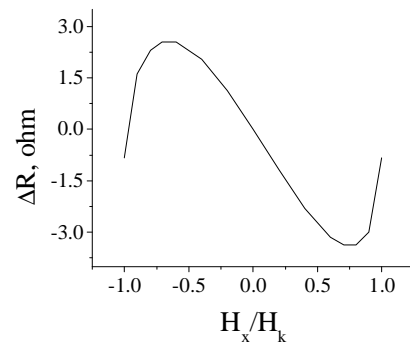


Fig. 10. Change of the total resistance  $\Delta R$  at mixed in parallel BP and MR effects.

#### 4. Results and discussion

The perfect barber pole response is characterized by equal absolute values of the maximum increase of the resistance ( $\Delta R_{\max}$ ) at the one polarity of the applied field and of the maximum decrease ( $\Delta R_{\min}$ ) at the opposite polarity (with respect to  $R(0)$ ). For perfect anti-symmetry  $(\Delta R_{\max})/(\Delta R_{\min}) = 1$ , falling to zero with deterioration of the effect. If one accepts  $(\Delta R_{\max})/(\Delta R_{\min})$  as a criterion for the quality of the effect, the dependences shown in Figs. 11 and 12 can be deduced from the above considerations. In Fig. 11, the dependence of  $(\Delta R_{\max})/(\Delta R_{\min})$  on the percentage of working contacts is presented. It is seen that a very high degree of effectiveness and reliability of the contacts is needed in order to obtain at least some degree of anti-symmetry. On the other hand, the dependence of  $(\Delta R_{\max})/(\Delta R_{\min})$  on  $D/W$  is significantly more gradual. On the basis of these two dependences, and knowing the capacity of a specific technology (minimum dimensions of the openings and the shorting bars processed), a trade off could be made about the widths of the contacts and the distances between them.

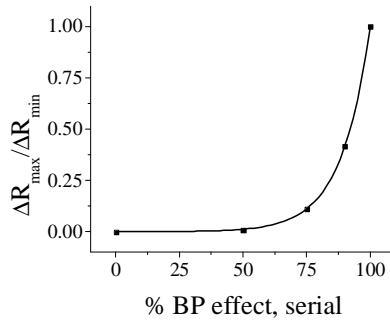


Fig. 11. Dependence of the quality of the BP effect on the percentage of good contacts.

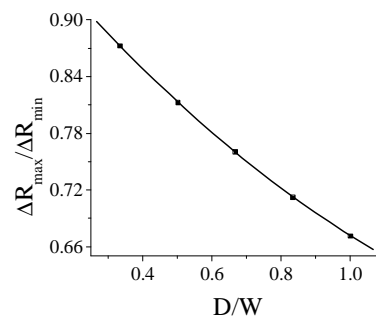


Fig. 12. Dependence of the quality of the BP effect on  $D/W$ .

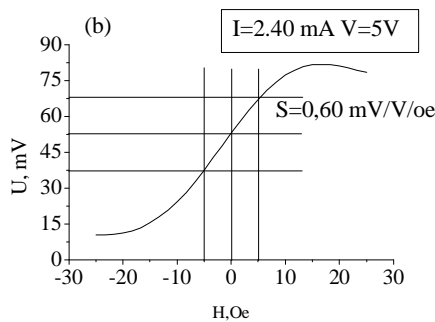


Fig. 13. Output signal of the produced BP bridge before cutting the wafer into dices.

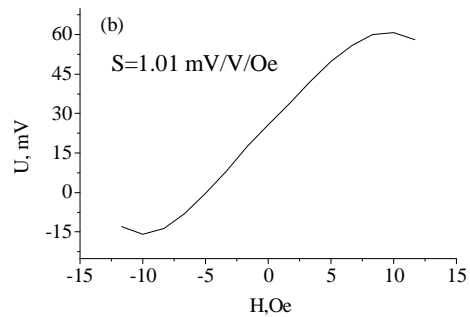


Fig. 14. Output signal of a BP bridge produced on a cut dice.

Making use of the conclusions drawn from the described model, and of a technology with magnetization of the magnetoresistive layer after annealing (described elsewhere [12]) a barber pole bridge based on permalloy was designed and produced. It consisted of four meander-shaped resistors, each containing 26 permalloy stripes. The barber pole structure was based on the ratio  $D/W = 2/3$ . The response of the bridge  $U$  (output signal in mV) to applied magnetic fields is shown in Figs. 13 and 14. In Fig. 13 a typical response on a wafer with chips is demonstrated. In Fig. 14 a typical example of the response of devices from the same batch, but already diced, is shown. It is seen that the sensitivity is increased by almost a factor of two. It is found that on the wafer, chips behave magnetically like one entity with a higher  $H_k$  and a higher stability (thus lower sensitivity). The already diced and packaged chips can be used for capturing magnetic fields for the purposes of

automation. Two chips mounted in one package and rotated at  $90^\circ$  can be used for angle measurements in the range  $0-360^\circ$ .

In parallel, single-stripe magnetoresistors were implemented on sital (a glazed ceramic) substrates. Sital was chosen among several tested types of ceramics used in thick film technology. It proved to be the only material among them with sufficient smoothness to give a high-quality AMR effect. The devices produced demonstrated  $\delta\rho/\rho = 2.50-2.66\%$ . Also, sital is easily processed by laser technology (different shapes of the substrate, drilling holes through it). The obtained results could be used for implementing application-specific devices with different shapes, integrated with CMOS chips for data processing.

## 5. Conclusions

The structure of the AMR devices and the AMR technology are flexible and compatible with conventional IC technology (CMOS in particular). By careful estimation of the main risks and trade-offs, single-stripe and barber pole AMR devices could be produced using equipment which is conventional for the microelectronics industry, without any upgrading. Sital is a very good material as a substrate for AMR devices. It is readily processed by laser technologies and suitable for the flexible design and production of application-specific subsystems integrating AMR devices and CMOS chips.

## References

- [1] S. Tumanski, "Thin Film Magnetoresistive Sensors", IOP Publishing Ltd, U.K. (2001).
- [2] Honeywell, Product specification - HMC1001/1002; HMC1021/1022.
- [3] Honeywell, Product specification - HMC1051Z/HMC1052.
- [4] Philips, Product specification - KMZ51.
- [5] Philips, Product specification - KMZ41.
- [6] J. Smit, *Physica* **17**, 612 (1951).
- [7] A. Marsocci, *Phys. Rev.* **137**, 1842 (1965).
- [8] G. Thomas, *Physica* **45**, 407 (1969).
- [9] E. Kuijk, *IEEE Trans. Magn.* **11**, 1215 (1975).
- [10] E. Kuijk, Magnetoresistive magnetic head, US Patent 4 052 748.
- [11] W. Gorter, Magnetoresistive magnetic head, US Patent 4 040 113.
- [12] S. Andreev, J. Koprinarova, P. Dimitrova, *J. Optoelectron. Adv. Mater.* **7**(1), 317 (2005).